Lipid composition of integral purple membrane by ^{1}H and ^{31}P NMR

Christian Renner,[1] Brigitte Kessler, and Dieter Oesterhelt

Max-Planck-Institut für Biochemie, 82152 Martinsried, Germany

Abstract **In the purple membrane (PM) of halobacteria, lipids stabilize the trimeric arrangement of bacteriorhodopsin (BR) molecules and mediate the packing of the trimers in a regular crystalline arrangement. To date, the identification and quantification of these lipids has been based either on lipid extraction procedures or structural models. By directly solubilizing PMs from *Halobacterium salinarum* in aqueous detergent solutions (SDS or Triton X-100), we avoided any separation or modification steps that might modify the lipid composition or even the lipid molecules themselves. Our analysis of integral PM preparations should resolve partially conflicting literature data on the lipid composition of the PM. Using ^{31}P and ^{1}H NMR of detergent-solubilized but otherwise untreated samples, we found two glycolipids and 6.4 ± 0.1 phospholipids per BR molecule, 4.4 ± 0.1 of the latter being the phosphatidylglycerophosphate methyl ester. The only glycolipid detected was S-TGD-1. For an additional glycolipid, glycocardiolipin, that was recently identified in lipid extracts, we show that it was produced mainly during the lipid extraction procedure but also was partially dependent on the preparation of the PM suspensions.—** Renner, C., B. Kessler, and D. Oesterhelt. **Lipid composition of integral purple membrane by ^{1}H and ^{31}P NMR. *J. Lipid Res.* 2005.** 46: **1755–1764.**

Supplementary key words phospholipids • glycolipids • nuclear magnetic resonance • bacteriorhodopsin

Lipids as constituents of cellular membranes play a role at least as fundamental for living organisms as proteins and nucleic acids. They define the inside and outside of a cell and thus the existence of a cell as such. The physical properties of lipid bilayers allow the incorporation of functional units mostly built up from proteins for energy production, communication, material transport, and many other vital tasks. The cell membrane of *Halobacterium salinarum* contains specialized patches called purple membrane (PM) that consist of two-dimensional crystalline arrays of the protein bacteriorhodopsin (BR), which is a light-driven proton pump (1, 2). In the PM, BR forms trimers that are placed on a crystal lattice. Both the trimerization and the formation of the crystalline patches require lipid molecules at defined positions (3–5). Because of their high fluidity, natural membranes are generally of fluctuating heterogeneity and thus difficult to study. The PM, with its regular structural arrangement, is a remarkable exception and therefore has served as a model system for the investigation of membrane proteins and lipid-protein interactions. Whereas the three-dimensional structure of BR has been the focus of intense research for decades, the lipids of the PM have received considerably less attention. Early efforts to determine the lipid content of PM consisted of spatial considerations based on the size of the crystal unit cell (6). These early estimations (10 lipids per BR) proved consistent with later electron diffraction data and were used in the construction of an atomic model of PM (7). Detection and identification of TLC-separated lipids from PM lipid extracts gave a more detailed view of the lipid composition of PM (8, 9). Besides the main component phosphatidylglycerophosphate methyl ester (PGP-Me), phosphatidylglycerol (PG), phosphatidylglycerosulfate (PGS), the glycolipid STGD-1, and the neutral lipids squalene and vitamin MK-8 also were found. In structural studies, some of the lipid molecules could be observed directly as a result of their apparently well-ordered positions inside and outside the BR trimers (3–5). Although approximately one-third of the lipids can be removed without observable changes in the PM structure (3), PM function is reduced by such treatment (10). Besides the structural role, a functional character as a selective K^{+} receptor was proposed for the glycolipid (11).

Recently, the lipid composition of PM was reinvestigated (12, 13) with surprising results. Two new lipid components were identified and, because of their similarity to eukaryal cardiolipins, termed achaeal glycocardiolipin (GlyC) and achaeal cardiolipin (BPG). Whereas GlyC accounted for 10% of the total lipid molecules, BPG was found only in minor amounts and, in fact, had already been observed in the PM of *H. halobium* (now called *H. salinarum*) by a Russian group (14). The early publications of Ushakov et al. (14)

Manuscript received 8 April 2005 and in revised form 10 May 2005.

Published, JLR Papers in Press, June 1, 2005.
DOI 10.1194/jlr.M500138-JLR200

[1] To whom correspondence should be addressed.
e-mail: renner@biochem.mpg.de

and Chekulaeva, Tsirenina, and Vaver (15) on the lipid composition of halobacteria and specifically the PM of *H. halobium* were unfortunately published in Russian (without English translation) and therefore have been completely overlooked by the non-Russian literature. **Figure 1** displays the chemical structure of the polar lipids that have been reported as contained in the PM (8, 9, 11, 12, 14, 15).

In the present study, we set out to analyze the lipids of the PM, avoiding any separation, extraction, or purification steps to retain the unmodified lipids in their original amounts.

MATERIALS AND METHODS

Sample preparation

Patches of PM were extracted from cells of the *H. salinarum* S9 strain as described (16). BR concentrations were determined via absorption at 568 nm using an absorption coefficient of 63,000 M^{-1} cm^{-1} for the light-adapted state containing 100% all-*trans* retinal (17). A suspension of optical density 20 was solubilized by the addition of 10% Triton X-100, 10% SDS, or 10% fully deuterated-SDS. In the case of Triton, the purple color was retained, indicating the presence of intact BR, whereas SDS leads to denaturing of the protein accompanied by a loss of color to slightly yellowish. For NMR measurements, BR was diluted with pure water to final concentrations of between 3 and 300 μM. Each NMR sample contained 10% D_2O for lock stabilization and, unless stated otherwise, 5 mM hexamethylphosphoramide (HMPA) and EDTA in a 20-fold concentration compared with BR. For ^{31}P NMR measurements, EDTA is essential for avoiding line broadening as a result of divalent metal cations (18). For glycolipid determination, the final PM purification step using a sucrose gradient had to be avoided, because residual sucrose would completely cover the sugar signals from glycolipids in ^1H NMR. Instead, the lysate was centrifuged for 10 min at 48,000 *g*. Then, the pellet was resuspended in water and recentrifuged, selecting only the largest patches of PM. To reduce the water signal in ^1H NMR, PM was washed several times with D_2O. Deuterated SDS as well as EDTA and HMPA from stock solutions prepared with D_2O were added. The final volume was 474 μl for all samples.

Lipid extraction

Extraction of lipids from PM preparations was performed according to four different protocols, the first three being modifications of the original Bligh and Dyer (19) procedure using 1:2:0.8 (v/v) chloroform-methanol-water mixtures for the initial extraction step. Protocol 2 was identical to that used by Corcelli et al. (13), including centrifugation after extraction and the addition of benzene before final drying with N_2. Protocol 1 differed from the others in that the extraction was performed under acidic conditions (5 mM citric acid) and brought to dryness at increased temperature (40°C) after treatment with Na_2SO_4. Protocols 1 and 3 do not use separation by centrifugation. Before phase separation, water and chloroform were added to final $CHCl_3$- MeOH-water ratios of 2:2:1.8, 1.5:2:1.3 and 2:2:0.8 for protocols 1, 2, and 3, respectively, with protein concentrations of 0.09, 0.13, and 2.0 mg/ml at this step. In protocol 4, extraction was achieved simply by adding to a PM suspension (1 mg/ml) twice the volume of ethanol. After centrifugation, the supernatant was directly dried with air.

For ^{31}P NMR, lipid extracts were dissolved either in water containing 3% fully deuterated-SDS or in a mixture of chloroform, methanol, and water (10:4:1, v/v). EDTA was added in both cases. For the latter mixture, Cs-EDTA was used because of the poor solubility of Na-EDTA in organic solvents, and after phase separation only the chloroform phase was placed in the active volume of the receiver coil.

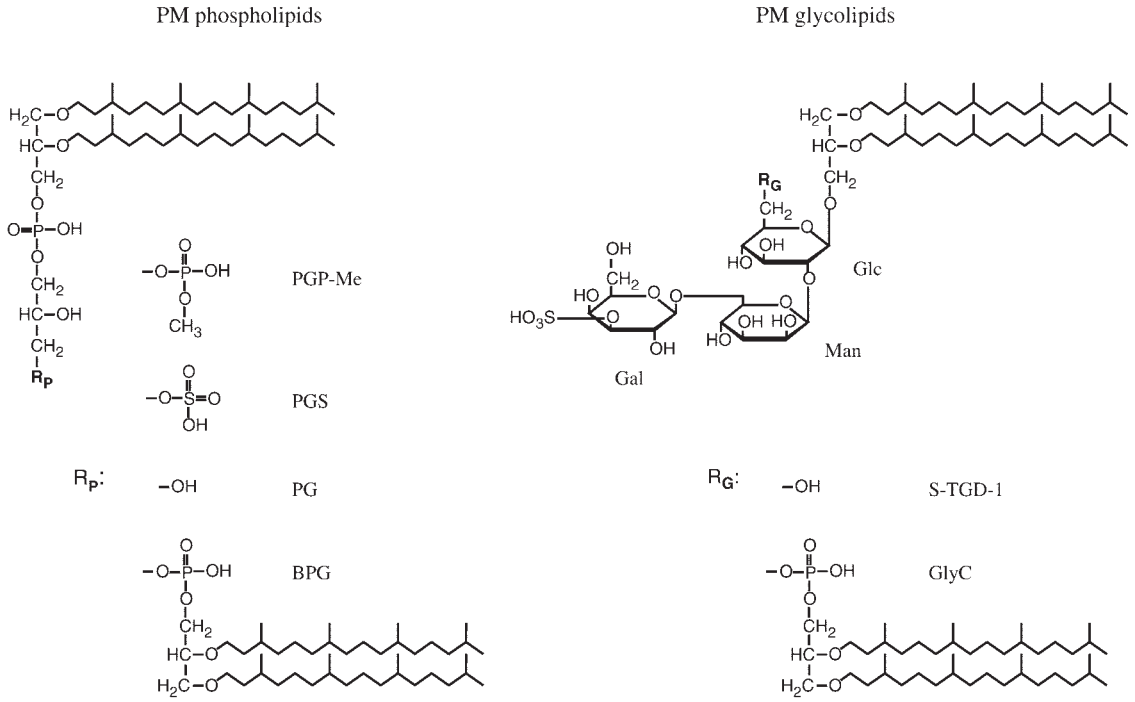

Fig. 1. Chemical structure of the purple membrane (PM) polar lipids. BPG, achaeal cardiolipin; GlyC, glycocardiolipin; PG, phosphatidylglycerol; PGP-Me, phosphatidylglycerophosphate methyl ester; PGS, phosphatidylglycerosulfate.

Thin-layer chromatography

TLC of lipid extracts was performed on silica gel 60A plates (Merck, Darmstadt, Germany) in a chloroform-methanol-90% acetic acid mixture (65:4:35, v/v). For detection, TLC plates were heated after application of 20% H_2SO_4 in ethanol.

NMR measurements

NMR experiments were performed at 300 Kelvin (K) on Bruker DRX500 and AMX400 spectrometers using 5 mm broadband inverse and TXI probes with z-gradient equipment. For the quantification of ^{31}P NMR signals, a 30 s relaxation time between scans was chosen to allow for full relaxation of all ^{31}P nuclei (T_1 of HMPA was ~6 s under the conditions chosen here; the lipids relaxed faster with T_1 = 1.4 s for the high-field and T_1 = 2.7 s for the low-field resonances). Several one-dimensional ^{31}P spectra with ^1H decoupling, typically with 1,024 scans each, were recorded for each sample. Three hertz (Hz) exponential line broadening and polynomial baseline correction were applied before the integration of spectra. ^{31}P spectra without ^1H decoupling and with narrow-band selective ^1H decoupling were used together with two-dimensional ^1H-^{31}P correlation spectra to assign the phospholipid signals. Specifically, ^{31}P HSQC (20) with transfer delays corresponding to a 15 Hz coupling constant and HSQC-TOCSY experiments with an additional 70 ms MLEV-17 (21) mixing period for protons after the HSQC step were performed. ^{31}P chemical shifts were calibrated to 0 ppm for 80% H_3PO_4 by placing the 5 mm PM sample tubes into a 10 mm NMR tube filled with 80% H_3PO_4 in water. D_2O of the inner sample tube was used as lock signal, and the ^{31}P resonances of phosphoric acid in the outer volume and HMPA in the inner tube were detected simultaneously in one spectrum. Direct calibration with 80% H_3PO_4 as an external reference had to be performed for each solvent system (SDS, Triton), because HMPA and D_2O chemical shifts differ slightly for different detergent systems and concentrations. The disadvantage of indirect calibration via two separate measurements of external reference and sample is that the lock substance (D_2O) experiences slightly different shifts in the different environments (e.g., 80% H_3PO_4 vs. 10% SDS). Measuring reference and sample signal in one experiment avoids this problem as well as all other possible differences (e.g., in temperature) associated with separate measurements.

The glycolipid content of PM solubilized with deuterated SDS was estimated from one-dimensional ^1H spectra. The PM used for these measurements was washed several times with D_2O (see above), and HMPA and EDTA stock solutions were prepared with D_2O as well to minimize the residual water signal. In this case, 20 s between scans were sufficient for full ^1H relaxation (nonselective T_1 of HMPA was 2.7 s, but the residual protons of the deuterated SDS-micelles relaxed more slowly with $T_1 \sim 4$ s, and saturation transfer had to be avoided). One hertz line broadening was used. Manual baseline correction was performed separately for each spectral region containing a signal of interest. In this regard, the background of broad signals originating from solubilized BR was treated as baseline. Two-dimensional TOCSY (21) and two-dimensional ^1H-^{13}C HSQC experiments (20) were recorded to verify the assignment of the anomeric proton signals and to show that no other narrow signals overlap. To this end, TOCSY mixing times up to 200 ms were used as a filter for narrow lines because relaxation efficiently reduces broad protein signals during this mixing period. In the TOCSY experiment, weak presaturation (4 Hz field strength) was used to suppress the residual water signal. Spectral width was 12 ppm centered on water for both dimensions. The two-dimensional ^1H-^{13}C HSQC used coherence pathway selection by gradient pulses (22). For the proton spectral width, 14 ppm centered on water was chosen, whereas for ^{13}C, 130 ppm around a carrier frequency of 70 ppm was used.

For ^1H and ^{31}P diffusion measurements, stimulated echo experiments with bipolar gradients and diffusion times between 20 and 500 ms were performed with different gradient strengths between 1 and 60 Gauss (G)/cm. The gradient strength was calibrated to a diffusion constant of 18.7×10^{-10} m^2/s for water in D_2O at 300 K. Only well-resolved signals were used to extract diffusion constants from the monoexponential signal decay. ^{31}P as well as ^1H T_1 relaxation times were determined by saturation recovery experiments at different PM concentrations and in the absence and presence of EDTA.

Spectra processing

Spectra were processed and evaluated using XWINNMR 3.0 (Bruker Biospin). For each sample, the content of phospholipids was determined by integration of signals in the ^{31}P spectrum and comparison with the HMPA signal that corresponded to 5 mM phosphorus. Values from several spectra were averaged, and the standard deviation was taken as the experimental measurement error. The statistical error as expressed in signal-to-noise ratios

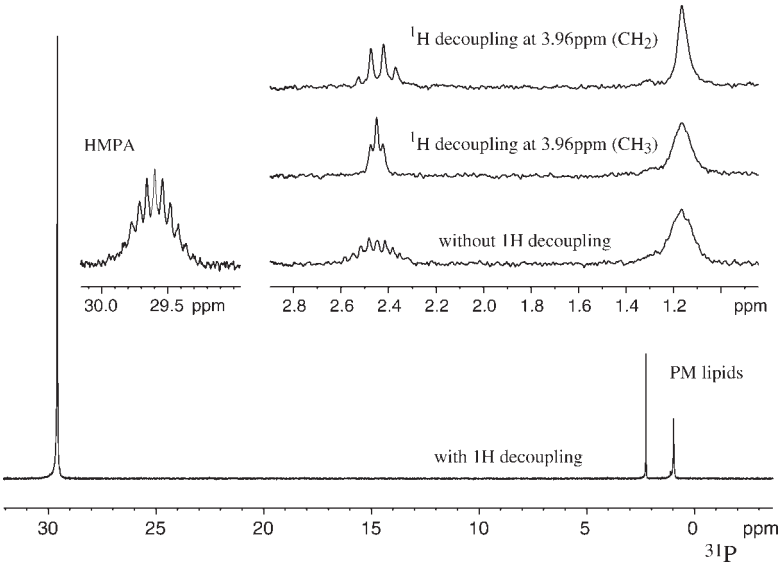

Fig. 2. ^{31}P NMR spectra of PM solubilized by the addition of 10% deuterated SDS. The addition of EDTA is crucial for obtaining narrow lipid resonances. Selective ^1H decoupling allows the assignment of the low-field lipid resonance as originating from PGP-Me only, whereas the high-field signal consists of multiple overlapping peaks. HMPA, hexamethylphosphoramide.

generally accounted for only part of the total measurement error for these spectra. Systematic errors result from spectra processing (phasing, baseline correction) as well as from spectrometer instabilities (temperature, field homogeneity, electronics). Therefore, the experimental measurement error cannot be reduced arbitrarily by accumulating more scans. Comparing the values for phospholipid content in the various samples shows that the standard deviation for the lipid-to-BR ratio across all samples is similar to the mean measurement error, meaning that variations between samples are smaller or in the same range as the experimental error for determining the phospholipid content. This internal check of data quality is important because precise measurements require highly reproducible samples.

RESULTS

Characterization of solubilized PM

In the preparation of the NMR samples from PM patches, we strictly avoided any separation steps such as centrifugation, purification, or phase separation that might selectively enrich or deplete the lipid content of the final sample. The only modifications compared with integral PM consisted of detergent and EDTA to allow NMR measurements as well as a small amount of HMPA as an internal standard. For the quantitative determination of lipid content, it is essential that not only all lipids of the original PM are contained in the NMR sample but also that all lipids are detected in the NMR measurement. This is especially important because we decided to determine the absolute concentrations of the lipids and compare them with the BR concentrations that were determined by ultraviolet-visible absorption spectra recorded before solubilization. The ratio of both concentrations yielded the desired stoichiometry. As intensity reference for ^{1}H as well as ^{31}P, we used HMPA at a fixed concentration of 5.0 mM, because no suitable and reliable reference signal in the NMR spectra of solubilized PM could be found. The chemical shift of HMPA and the NMR detection efficiency (signal intensity/concentration) were found to be concentration-independent. Together with the fact that ^{1}H and ^{31}P signals of HMPA are well resolved in the spectra of samples containing solubilized PM, this qualifies HMPA as a suitable reference compound. Long T_1 times and large diffusion constants show that HMPA does not interact with the detergent (SDS or Triton) but remains in the bulk water phase. Diffusion constants for HMPA determined by ^{1}H NMR ($D_{HMPA}^{1H} = 1.7 \times 10^{-10}$ m^2/s) and ^{31}P NMR ($D_{HMPA}^{31P} = 1.8 \times 10^{-10}$ m^2/s) agree well and allow comparison with lipids that are only observable in the ^{31}P spectrum ($D_{lipids}^{31P} = 0.6 \times 10^{-10}$ m^2/s) and BR that is present only in the ^{1}H spectrum ($D_{BR}^{1H} = 0.4 \times 10^{-10}$ m^2/s). The diffusion of lipids and BR is similar to that of SDS ($D_{SDS}^{1H} = 0.5 \times 10^{-10}$ m^2/s), indicating the insertion or inclusion of the hydrophobic parts of both molecules (lipid chain and transmembrane helices, respectively) inside detergent micelles. T_1 relaxation times of the ^{31}P signals from lipids and HMPA were determined for all samples. Interestingly, a strong dependence on the presence of EDTA in the

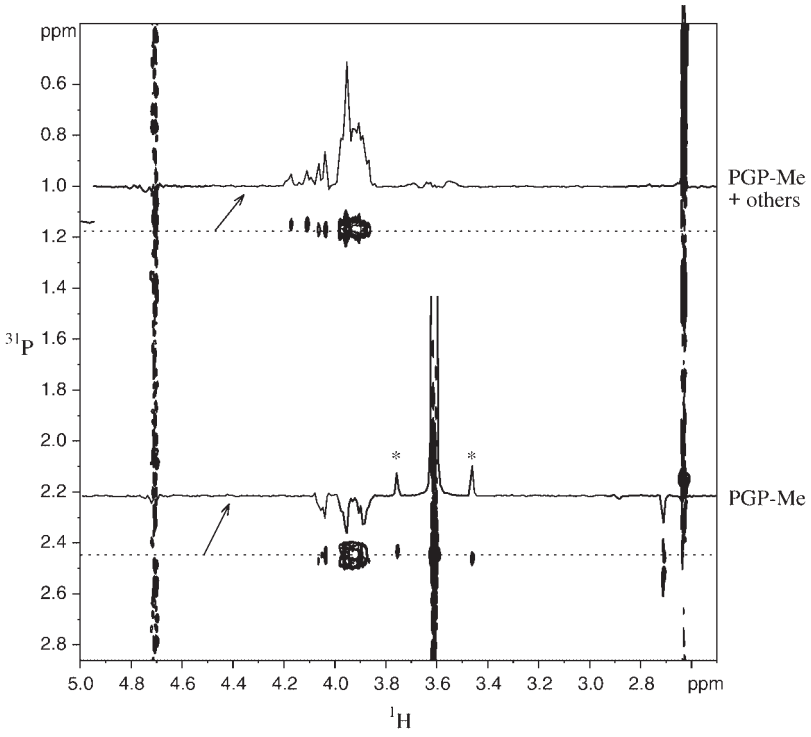

Fig. 3. ^{1}H-^{31}P HSQC-TOCSY spectrum of deuterated SDS-solubilized PM. Dotted lines indicate the positions of the one-dimensional slices displayed above the cross-peaks. ^{13}C satellites of the cross-peak corresponding to the coupling between the methyl and phosphate group of PGP-Me are marked by asterisks. The trace at 2.6 ppm originates from the HMPA cross-peak that is multiply folded.

sample was observed. ^{1}H T_1 times for HMPA and SDS approximately doubled upon addition of EDTA, whereas the ^{31}P T_1 time for HMPA increased by a factor of seven. The ^{31}P line widths of the two lipid signals decreased dramatically from ~30 and ~60 Hz to 2.5 and 10 Hz for the low-field and high-field signals, respectively. The addition of larger amounts of EDTA was without effect on line width. The necessity to use EDTA in ^{31}P NMR of phospholipids is well known (18). By charge-charge interactions with the phosphate groups, metal ions probably induce the aggregation of phospholipids, leading to the observed line broadening that can be removed upon capture of the ions by the metal-chelating EDTA. For organic solvents, the cesium salt of EDTA was proposed because of its better solubility in apolar media (18). In aqueous solutions, the solubility of the sodium salt of EDTA is no issue.

Resonance assignment

In the ^{31}P NMR spectra of solubilized PM, two signals from phospholipids were observed (**Fig. 2**). For both signals, coupling to a number of protons was detected via two-dimensional ^{31}P-^{1}H HSQC and HSQC-TOCSY (**Fig. 3**). Although the two-dimensional ^{31}P-^{1}H HSQC correlates the ^{31}P frequency (*y* axis in Fig. 3) with the proton frequencies of directly coupling hydrogens, the two-dimensional ^{31}P-^{1}H HSQC-TOCSY yields the full ^{1}H spin system in the proton dimension (*x* axis in Fig. 3). Characteristic patterns in these two-dimensional spectra allow the discrimination of lipids even if ^{31}P resonances overlap. In one-dimensional ^{31}P NMR spectra, selective narrow-band decoupling showed that the low field signal was coupled to a CH_3 group with a proton chemical shift of 3.6 ppm and a CH_2 group resonating at 4.0 ppm (Fig. 2). The only phospholipid known to occur in PM with a methyl group linked directly to the phosphate is the PGP-Me (8, 12). Therefore, the low field signal at 2.45 ppm was unambiguously assigned to PGP-Me. The selective decoupling experiments as well as the narrow line width (2.5 Hz) exclude the possibility of overlap for this signal. Contrarily, the phosphorus signal at 1.2 ppm clearly consists of several resonances. A part of the signal that corresponds in intensity exactly to the 2.45 ppm signal must stem from PGP-Me, as this phospholipid contains two phosphate groups (that are chemically not equivalent). The difference of 1.2 ppm between the two PGP-Me resonances agrees very well with literature values (13). The absolute shifts, however, differ, as a different solvent system was used. Besides the PGP-Me that makes up most of the high field signal, at least two other resonances contribute. Because these resonances can be neither separated nor assigned, they are collectively referred to as "others."

The assignment of glycolipids was based on the previous work of Corcelli et al. (12). A two-dimensional ^{13}C-^{1}H HSQC (**Fig. 4**) that correlates carbon chemical shifts with the proton frequencies of directly bonded hydrogens revealed the presence of three anomeric carbons/protons at positions almost identical to those reported. The inset in Fig. 4 demonstrates that no other resonances (e.g., from BR) are close to the anomeric signals, allowing the assignment of these peaks to the glycolipids. Because of their narrow line width, the anomeric proton signals identified in the HSQC can also clearly be seen in the one-dimensional ^{1}H spectra of samples prepared with D_2O and deuterated SDS, albeit very close to the residual water signal (**Fig. 5**). A two-dimensional TOCSY experiment with an extremely long mixing time (200 ms; **Fig. 6**) that con-

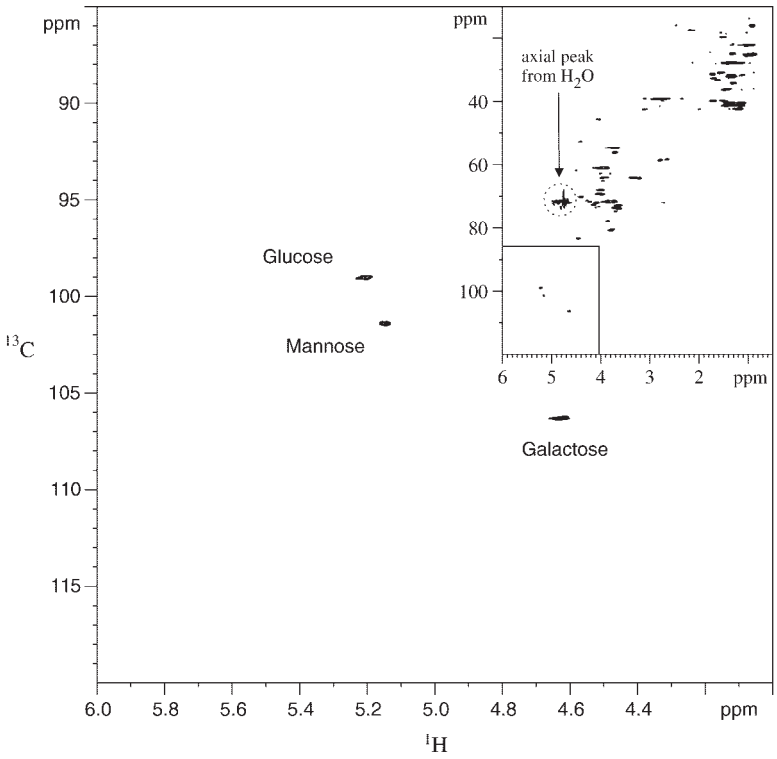

Fig. 4. Part of the ^{1}H-^{13}C HSQC spectrum of deuterated SDS-solubilized PM containing the anomeric signals of the glycolipids. The inset displays an overview showing resonances from bacteriorhodopsin and detergent.

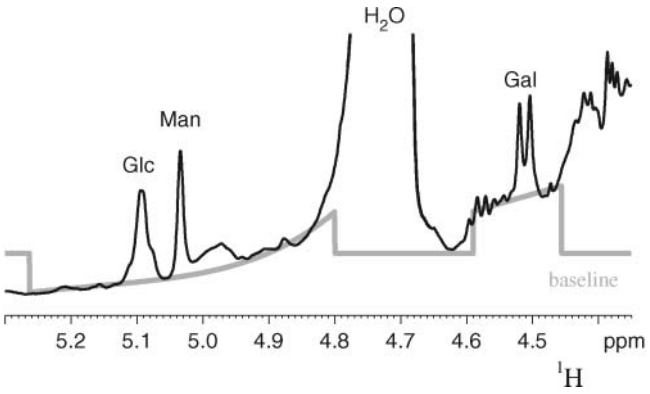

Fig. 5. Section of the one-dimensional ^{1}H spectrum of deuterated SDS-solubilized PM prepared in D_2O showing the anomeric glycolipid signals. The manually adjusted polynomial baseline is shown together with the uncorrected spectrum.

nects all proton NMR frequencies within a given spin system was performed to selectively observe narrow lines from sugar moieties as broad lines (from the protein or the lipid chains) that are strongly reduced during the long mixing period as a result of their much faster transverse relaxation. The assignment of the anomeric signals

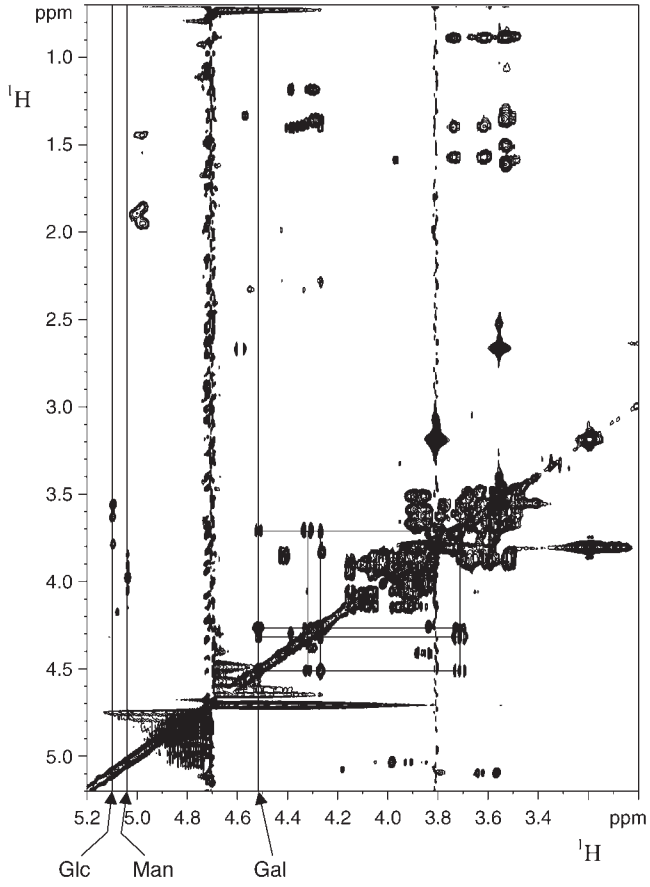

Fig. 6. Aliphatic part of the two-dimensional ^{1}H TOCSY spectrum of deuterated SDS-solubilized PM in D_2O. Most protein and detergent signals are suppressed by a long mixing time of 200 ms. The spin system of galactose is indicated by lines.

TABLE 1. Phospholipid content in solubilized PM determined by ^{31}P NMR

Detergent	PM Concentration[a]	Number of Phospholipids per BR Molecule	
		PGP-Me[b]	Others[b]
	μM		
Triton X-100	266	4.70 ± 0.07	1.98 ± 0.13
	133	4.49 ± 0.31	2.26 ± 0.36
SDS	266	4.49 ± 0.16	2.10 ± 0.23
	133	4.19 ± 0.24	2.20 ± 0.66
Deuterated SDS	266	4.68 ± 0.06	1.80 ± 0.13
	266	4.71 ± 0.13	1.51 ± 0.20
	133	4.45 ± 0.18	1.52 ± 0.24
	66	4.22 ± 0.39	1.89 ± 0.57
	66	4.27 ± 0.33	2.27 ± 0.45
	33	3.74 ± 0.41	2.49 ± 1.01
Average ± error[c]		4.4 ± 0.1	2.0 ± 0.1
Standard deviation across all samples		0.28 (6%)	0.31 (16%)

BR, bacteriorhodopsin; PGP-Me, phosphatidylglycerophosphate methyl ester; PM, purple membrane.

[a] 15.87 μM PM = optical density of 1; all samples were from the Max-Planck-Institut für Biochemie.

[b] Average and standard deviation are calculated from 4 to 12 separate measurements.

[c] The error in the average is the standard deviation divided by the square root of the number of samples.

as originating from sugar groups is confirmed by the observation of spin systems that are typical for sugars but that do not occur for any amino acid residue. As an example, the spin system of galactose is indicated in Fig. 6.

Phospholipid content

Complete solubilization of PM by the detergents used is indicated by a lack of concentration dependence of phospholipid contents, as shown in **Table 1**. Very careful sam-

TABLE 2. Glycolipid content in fully deuterated-SDS-solubilized PM determined by ^{1}H NMR

PM Concentration[a]	Number of Glycolipids per BR Molecule[b] (Average ± Standard Deviation)[c]		
	Galactose	Mannose	Glucose
mM			
266	1.71 ± 0.25	1.7 ± 0.1	2.6 ± 0.1
133	2.10 ± 0.08	1.7 ± 0.2	2.5 ± 0.3
66	2.07 ± 0.14	2.1 ± 0.1	2.6 ± 0.2
33	1.91[d]	2.2[d]	1.9[d]
13	1.84 ± 0.12	2.6 ± 0.5	2.1 ± 0.4
2.7	1.27 ± 0.15[e]	—	—
Average ± error[f]	1.9 ± 0.1	2.0 ± 0.1	2.5 ± 0.1
Standard deviation across all samples	0.18 (10%)	20%	15%

[a] 15.87 μM PM = optical density of 1; all samples were from the Max-Planck-Institut für Biochemie.

[b] The most reliable measurements were performed using the galactose signal; for mannose and glucose, systematic baseline errors were more severe.

[c] Average and standard deviation are calculated from four to seven measurements using two or three different samples.

[d] Only one measurement was performed.

[e] Not included in the average of all samples.

[f] The error in the average is the standard deviation divided by the square root of the number of experiments.

ple preparation allowed us to reduce sample-to-sample variations to the level of the measurement's error of each individual sample. Different detergents (Triton X-100, SDS, and fully deuterated-SDS) and different PM preparations were used to demonstrate that the phospholipid content is independent of the solubilization procedure. The amount of all phospholipids except PGP-Me (called others) was obtained by subtracting the PGP-Me contribution (obtained from the low field signal at 2.45 ppm) from the integral of the high field signal. Obviously, PGP-Me makes up most of the phospholipid content, with ~4.5 lipid molecules per BR. All others (PG, GlyC, BPG, PGS) account for only 2.0 lipid molecules per BR. In this regard, BPG, with its two indistinguishable phosphate groups, has to be counted as two lipid molecules.

Glycolipid content

The determination of glycolipid content was possible only because of the fortunate fact that the anomeric signals from the sugars can be observed in the one-dimensional ^{1}H NMR spectrum even in the presence of BR and even though the lipids are solubilized by insertion in detergent micelles (Fig. 5). Apparently, and not surprisingly, the three sugar moieties rotate quite mobilely in the water phase, whereas the attached lipid chains are inserted into the SDS micelle. Triton X-100 was not available in deuterated form; therefore, only SDS (deuterated) could be used as a detergent. Even though stock solutions and PM were prepared in D_2O to minimize the residual water signal, baseline correction and integration of lipid signals became increasingly difficult for low PM concentrations. Still, the high sensitivity of one-dimensional ^{1}H NMR spectra allowed us to cover 2 orders of magnitudes in PM concentrations. **Table 2** summarizes the glycolipid content as obtained from a comparison of the anomeric proton signals of glucose, mannose, and galactose with the 5 mM HMPA signal as a reference. Approximately two glycolipid molecules per BR were observed. The galactose signal was the primary target for quantification, because its detection and baseline correction suffered least from the nearby water signal. Still, the other two signals were evaluated also as a check of consistency, except for the lowest concentration. The accuracy of the determined glycolipid content might be less than the 5% precision because of possible systematic errors in baseline correction. However, considering the difficulties introduced by the presence of background signals from protein, detergent, and solvent, the results are quite satisfying.

It has been proposed that in addition to STGA-1, GlyC also is present to a larger extent (one per BR) in PM (13). In the ^{1}H spectra shown here (Figs. 4–6), only one set of sugar signals is visible. Chemical shift differences for the sugar moieties of STGA-1 and GlyC have been reported to be very small (12), so it might be possible that they completely overlap in our solvent system. Contrarily, in the phosphorus spectra of PM lipids, GlyC exhibits a well-separated resonance, at least in the solvent mix used by Corcelli et al. (13). Using PM from Bari, Italy, and the same extraction protocol and solvent mix described previously (13), we obtained a ^{31}P NMR spectrum very similar to the published one (**Fig. 7C**). Dissolving the same lipid extract in aqueous detergent solution allows the transfer of the as-

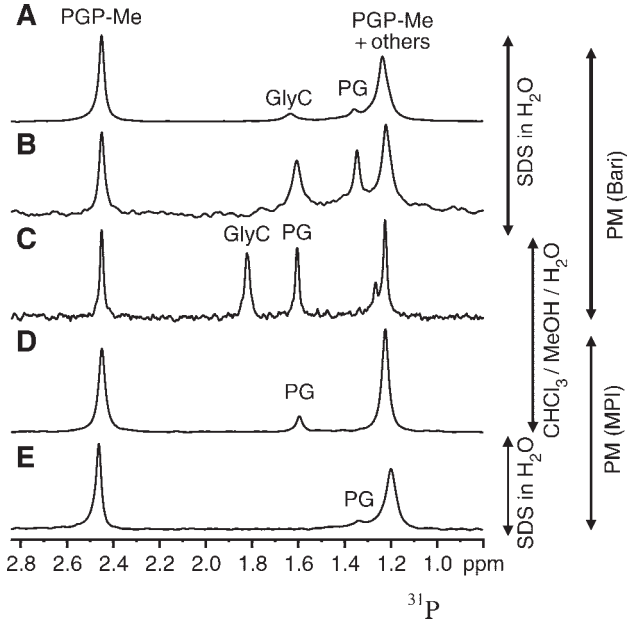

Fig. 7. ^{31}P NMR spectra of PM lipids. A, E: PM solubilized in 3% SDS in water. B–D: Lipid extract dissolved in either water/3% SDS (B) or chloroform-methanol-water ($CHCl_3$/MeOH/H_2O; 10:4:1, v/v) mixture (C, D). The PM preparation for A–C originated from Bari, Italy, and that for D, E was from the Max-Planck-Institut für Biochemie (MPI).

TABLE 3. Comparison with lipid contents of PM reported in the literature

PM Lipid	Present Work[a]	Corcelli et al. (13)[b]	Kushwaha, Kates, and Martin (8)[c]	Weik et al. (5)[d]	Grigorieff et al. (7)[e]
PGP-Me	4.4	2.4	3.7		
PG	~0.5[f]	1.2	0.3		
PGS + BPG	~1.5[f]	0.37	0.3[g]		
GlyC	—	1	—		
Phospholipids	6.4	5	4.3		
S-TGD-1	2	3	1.7		
GlyC	—	1	—		
Glycolipids	2	4	1.7	2	
Squalene	n.d.[h]	2	0.7		
Lipid chains	17[i]	20	13		20

BPG, achaeal cardiolipin; GlyC, glycocardiolipin; PG, phosphatidylglycerol; PGS, phosphatidylglycerosulfate. Lipid contents are reported relative to the BR concentration as molar ratios (number of lipids per BR molecule).

[a] NMR of solubilized PM.
[b] NMR of extracted lipids.
[c] Analysis of extracted lipids from PM of *H. cutirubrum*.
[d] Neutron diffraction of PM crystals.
[e] Electron diffraction, electron microscopy.
[f] The sum of PG, PGS, and BPG could be determined precisely to be 2.0, but the fraction of PG is only an estimation because of the overlap of ^{31}P NMR resonances. Note that BPG contributes double with its two phosphate groups.
[g] Only PGS was detected.
[h] n.d., not determined.
[i] Not including squalene.

signment of phosphorus signals to the micellar SDS solution (Fig. 7B–E). Obviously, signal dispersion in detergent micelles is smaller than in the organic solvent mix. However, GlyC is still well separated, and PG, although overlapping with other phosphate resonances, is still discernible. In Fig. 7A, it is demonstrated that direct solubilization of the Bari PM in 3% SDS yields a spectrum containing PG and GlyC only in comparatively small amounts. The strong influence of the extraction procedure is clearly visible. In all samples used for the determination of the lipid composition reported in **Table 3** (using PM prepared at the Max-Planck-Institut für Biochemie), no GlyC was detected from ^{31}P NMR (Fig. 7D, E). However, in a comparison of different extraction protocols, it was found for different PM preparations that each would yield at least small amounts of GlyC with some extraction protocols (**Fig. 8**).

DISCUSSION

A comparison of our results with previously published data is compiled in Table 3. In neutron diffraction studies of PM with deuterated sugar moieties, Weik et al. (5) had found two glycolipid molecules per BR, in perfect agreement with our data. Based on electron diffraction data, Grigorieff et al. (7) found space for 20 lipid chains (10 lipids per BR) in their structural model of PM, again well compatible with our number, especially considering that we could not detect squalene by the methods used. In the early studies of Kates and coworkers (8, 9), a very similar distribution of lipids was found for PM of *H. cutirubrum* as in the present work for PM of *H. salinarum*, albeit with a generally lower lipid content. Kates, Kushwaha, and Sprott (9) had observed only 2.6 molecules of retinal per BR trimer and explained that finding by degradation or incomplete extraction. However, assuming that their retinal extraction was complete, all lipids should be scaled up by a factor 3/2.6, resulting in numbers for the main components PGP-Me (4.3 per BR) and S-TDG-1 (1.9 per BR) that are indistinguishable from ours (4.4 and 1.9). From our data, only the sum of PGS and BPG is available. Assuming 0.3 molecules of PGS per BR, as reported by Kushwaha, Kates, and Martin (8), would lead to approximately one BPG per two BRs. The presence of BPG in the PM has been reported previously (12, 14).

Larger differences exist from recently published data (13) obtained by NMR of lipid extracts. Although the overall number of lipid molecules is similar, Corcelli et al. (13) observed a smaller amount of PGP-Me and increased amounts of PG and glycolipids compared with all other studies. Chemical modifications (see below) and selective enrichment or depletion of lipid species during the extraction procedure might cause some differences; therefore, we decided to avoid extraction and separation procedures for obtaining the natural lipid composition of unmodified PM.

The influence of the extraction procedure on the resulting lipid composition, especially the presence of GlyC, is clearly demonstrated in a comparison of extraction protocols (Fig. 8), in which no protocol produced GlyC from every PM preparation and no PM preparation yielded GlyC with every protocol. Apparently, subtle differences in the protocols of PM preparation or lipid extraction seem to be responsible for the production of GlyC. The erratic appearance of GlyC might be the reason why it had not been identified earlier, although, for example, it is clearly visible in a published mass spectrum of lipid extracts from PM used for the crystallization of BR [Fig. 1A in Essen et al. (4): m/z ($GlyC^{2-}$) = 966]. To exclude the presence of GlyC in directly solubilized samples, it has to be proven that no GlyC molecules can escape detection in the NMR experiment. The possibility that GlyC is not fully solubilized or is initially present but rapidly destroyed can be discarded on the basis of the spectra recorded from lipid extracts in aqueous detergent solution (Fig. 7B, C). Even ^{31}P NMR spectra of SDS-solubilized lipid extracts that were recorded after several months (without refrigerating the samples) exhibited no changes (data not shown), confirming the chemical stability of GlyC as well as the other phospholipids. Alternatively, one might suspect that GlyC resonances are shifted relative to the positions observed for solubilized lipid extract (Fig. 7B) (e.g., by binding to BR). In fact, GlyC is known to bind to BR in a specific manner in the intact PM. However, solubilization with SDS destroys the trimeric arrangement of BR as well as its native struc-

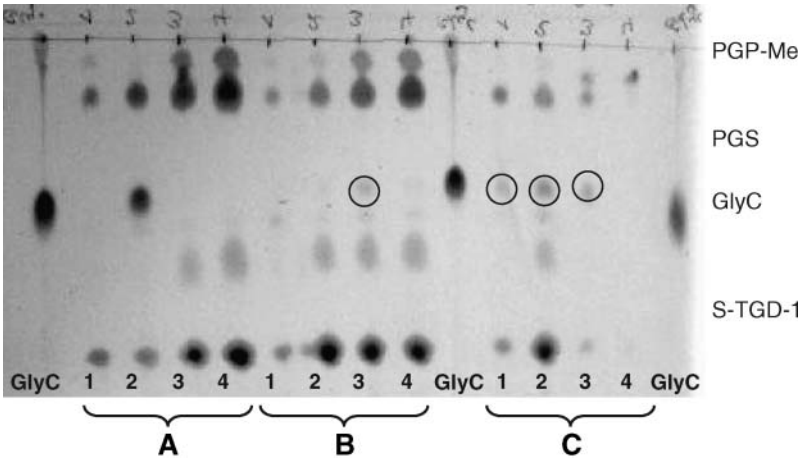

Fig. 8. TLC of lipid extracts from freshly prepared PM (A), frozen (−18°C) and stored (months) PM (B), and PM prepared in Bari, Italy (C). Four extraction protocols (lanes 1–4; see Materials and Methods) were tested for each PM, and purified GlyC was used as a reference. Weak GlyC spots are highlighted by black circles. The spots above and below GlyC originate from the other lipids.

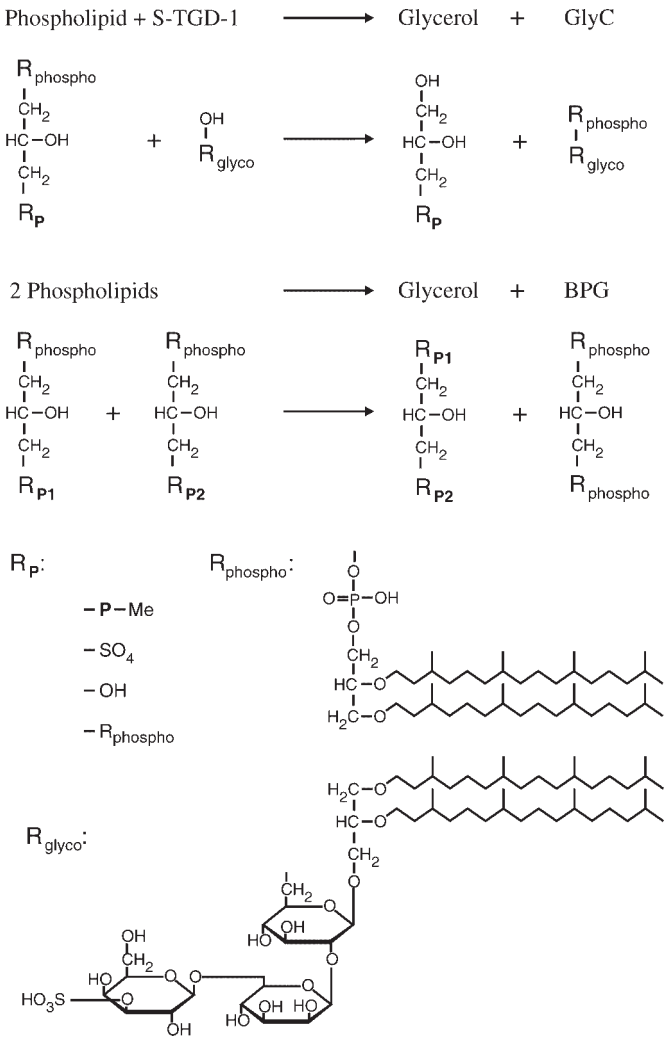

Fig. 9. Generation of GlyC and BPG by transesterification.

ture (see above), thereby abolishing the binding of GlyC. Furthermore, the two-dimensional ^{31}P-^{1}H correlation spectrum does not show the expected pattern that should be visible for GlyC in this spectrum, even if ^{31}P resonances completely overlapped. Finally, lipid extraction of solubilized PM did not result in detectable amounts of GlyC (data not shown). Therefore, it is certain that all GlyC present in the PM preparations is detected by the ^{31}P NMR spectra.

A comparison of different PM preparations (Figs. 7, 8) reveals that not only the lipid extraction but also the PM preparation itself can lead to the formation of GlyC, if only to minor extents. This aspect has been investigated in more detail recently and was related to osmotic shock (23).

Finally, it is tempting to speculate on the mechanism by which GlyC is generated. Figure 1 suggests that GlyC consists of the glycolipid S-TGD-1 with an extra phosphoglycerol moiety added at the glucose site. Considering that Corcelli et al. (13) found higher contents of GlyC and PG but less PGP-Me compared with the present work, a transesterification, as depicted in **Fig. 9**, seems possible. All phospholipids might produce GlyC or BPG in a reaction with glycerol derivatives as a second reaction product. Although the transesterification in total requires no energy, a considerable activation barrier has to be crossed. No generation of GlyC was observed in NMR samples kept at room temperature over periods of several months, clearly demonstrating that under equilibrium conditions transesterification occurs neither in aqueous detergent solution nor in the organic solvent mix. However, in the process of lipid extraction, the solvent change from water to organic solvents induces a sudden increase of Coulomb (electrostatic) interactions by the change of the dielectric constant. Together with the given spatial arrangement of the lipid molecules in the PM structure, the strongly increased electrostatic interactions might transiently catalyze and favor the formation of GlyC and BPG while the PM starts disintegrating. The following experimental observations support our hypothesis: *i*) solubilization with SDS detergent does not lead to the production of GlyC (Fig. 7) because the solvent dielectric constant does not change strongly; *ii*) lipid extraction of solubilized PM, in which the membrane structure is already destroyed, does not yield GlyC (data not shown); *iii*) the amount of GlyC generated is quite variable in similar extraction experiments (Fig. 8) because the catalytic process depends on the microscopic details of the lipid extraction procedure and PM disintegration that are difficult to control; *iv*) GlyC can be produced in the preparation of PM when the salt concentration (and concomitantly the electrostatic shielding) of cell membranes is strongly reduced by osmotic shock (23); and *v*) the number of GlyC molecules (one per BR) observed by Corcelli et al. (13) agrees with one accessible glycolipid per BR observed in neutron and X-ray scattering experiments (4, 5). The second glycolipid molecule per BR is well shielded from a spontaneous intramembrane chemical reaction because it is located and tightly bound inside the BR trimer (4). Although enzymatic activity in the reaction of a glycolipid with a phospholipid cannot decisively be excluded at present, the denaturing conditions during lipid extraction would favor a spontaneous chemical reaction under the given catalytic conditions detailed above. The unlikelihood of the chance occurrence of such a catalyzed transesterification could be taken as an indication that it may serve some purpose for halobacteria in the case of osmotic shock or low-salt conditions, as discussed previously (13, 23, 24). However, analyses should be performed on solubilized samples rather than lipid extracts, because in the latter case the extraction procedure can artificially increase the GlyC content.

Conclusions

By analyzing solubilized but otherwise untreated PM preparations, we determined the natural distribution of lipids in PM of *H. salinarum*, thereby resolving conflicting data from the literature. A recently discovered glycolipid, GlyC, was shown to be mostly a product of the lipid extraction procedure. To smaller extents, it can be generated during PM preparation by osmotic shock. However, GlyC is most likely not part of native PM.

We propose that it is generally more appropriate to analyze lipid compositions of membranes without separation

or extraction steps, as these procedures can selectively enrich, deplete, or, as shown here, even chemically modify lipids. We have demonstrated that in this respect NMR is an invaluable tool for the "integral" analysis of biological membranes as a result of the high resolution and multitude of nuclei that are available for observation.

The authors are grateful to Prof. Angela Corcelli, University of Bari, Italy, for the gift of PM as well as for insightful discussions.

REFERENCES

1. Oesterhelt, D., and W. Stoeckenius. 1973. Functions of a new photoreceptor membrane. *Proc. Natl. Acad. Sci. USA.* **70:** 2853–2857.
2. Oesterhelt, D. 1976. Bacteriorhodopsin as an example of a light-driven proton pump. *Angew. Chem. Int. Ed. Engl.* **15:** 17–24.
3. Grigorieff, N., E. Beckmann, and F. Zemlin. 1995. Lipid location in deoxycholate-treated purple membrane at 2.6 Å. *J. Mol. Biol.* **254:** 404–415.
4. Essen, L. O., R. Siegert, W. D. Lehmann, and D. Oesterhelt. 1998. Lipid patches in membrane protein oligomers: crystal structure of the bacteriorhodopsin-lipid complex. *Proc. Natl. Acad. Sci. USA.* **95:** 11673–11678.
5. Weik, M., H. Patzelt, G. Zaccai, and D. Oesterhelt. 1998. Localization of glycolipids in membranes by in vivo labeling and neutron diffraction. *Mol. Cell.* **1:** 411–419.
6. Blaurock, A. E., and W. Stoekenius. 1971. Structure of the purple membrane. *Nat. New Biol.* **233:** 152–154.
7. Grigorieff, N., T. A. Ceska, K. H. Downing, J. M. Baldwin, and R. Henderson. 1996. Electron-crystallographic refinement of the structure of bacteriorhodopsin. *J. Mol. Biol.* **259:** 393–421.
8. Kushwaha, S. C., M. Kates, and W. G. Martin. 1975. Characterization and composition of the purple membrane and red membrane from *Halobacterium cutirubrum*. *Can. J. Biochem.* **53:** 284–292.
9. Kates, M., S. C. Kushwaha, and G. D. Sprott. 1982. Lipids of purple membrane from extreme halophiles and of methanogenic bacteria. *Methods Enzymol.* **88:** 98–111.
10. Dracheva, S., S. Bose, and R. W. Hendler. 1996. Chemical and functional studies on the importance of purple membrane lipids in bacteriorhodopsin photocycle behavior. *FEBS Lett.* **382:** 209–212.
11. Falk, K. E., K. A. Karlsson, and B. E. Samuelsson. 1980. Structural analysis by mass spectrometry and NMR spectroscopy of the glycolipid sulfate from *Halobacterium salinarium* and a note on its possible function. *Chem. Phys. Lipids.* **27:** 9–21.
12. Corcelli, A., M. Coletta, G. Mascolo, F. P. Fanizzi, and M. Kates. 2000. A novel glycolipid and phospholipid in the purple membrane. *Biochemistry.* **39:** 3318–3326.
13. Corcelli, A., V. M. T. Lattanzio, G. Mascolo, P. Papadia, and F. Fanizzi. 2002. Lipid-protein stoichiometries in a crystalline biological membrane: NMR quantitative analysis of the lipid extract of the purple membrane. *J. Lipid Res.* **43:** 132–140.
14. Ushakov, A. N., M. L. Tsirenina, T. N. Simonova, S. K. Volkov, N. A. Koltovaya, L. N. Chekulaeva, and V. A. Vaver. 1978. Phospholipids of Halobacteria purple membranes. *Bioorg. Khim.* **4:** 774–781.
15. Chekulaeva, L. N., M. L. Tsirenina, and V. A. Vaver. 1980. Lipid composition of Halobacterium cells and bacteriorhodopsin isolated from them. *Ukrainskii Biokhim. Zhurnal.* **52:** 429–433.
16. Oesterhelt, D., and W. Stoeckenius. 1974. Isolation of cell membrane of *Halobacterium halobium* and its fractionation into red and purple membrane. *Methods Enzymol.* **31:** 667–678.
17. Oesterhelt, D., and B. Hess. 1973. Reversible photolysis of purple complex in purple membrane of *Halobacterium halobium*. *Eur. J. Biochem.* **37:** 316–326.
18. Meneses, P., and T. J. Glonek. 1988. High resolution ^{31}P NMR of extracted phospholipids. *J. Lipid Res.* **29:** 679–689.
19. Bligh, E. G., and W. J. Dyer. 1959. A rapid method of total lipid extraction and purification. *Can. J. Biochem. Physiol.* **37:** 911–917.
20. Bodenhausen, G., and D. J. Ruben. 1980. Natural abundance nitrogen-15 NMR by enhanced heteronuclear spectroscopy. *Chem. Phys. Lett.* **69:** 185–189.
21. Bax, A., and D. G. Davis. 1985. MLEV-17 based two dimensional homonuclear magnetization transfer spectroscopy. *J. Magn. Reson.* **65:** 355–360.
22. Davis, A. L., J. Keeler, E. D. Laue, and D. Moskau. 1992. Experiments for recording pure-absorption heteronuclear correlation spectra using pulsed field gradients. *J. Magn. Reson.* **98:** 207–216.
23. Lobasso, S., P. Lopalco, V. M. T. Lattanzio, and A. Corcelli. 2003. Osmotic shock induces the presence of glycocardiolipin in the purple membrane of *Halobacterium salimarum*. *J. Lipid Res.* **44:** 2120–2126.
24. Lopalco, P., S. Lobasso, F. Babudri, and A. Corcelli. 2004. Osmotic shock stimulates de novo synthesis of two cardiolipins in an extreme halophilic archaeon. *J. Lipid Res.* **45:** 194–201.